The Ternary System Nickel-Silicon-Titanium Revisited

Franz Weitzer, Masaaki Naka, Natalya Krendelsberger, Frank Stein, Cuiyun He, Yong Du, Julius C Schuster

Zeitschrift für Anorganische und Allgemeine Chemie

The Ternary System Nickel-Silicon-Titanium Revisited

Journal:	*Zeitschrift für Anorganische und Allgemeine Chemie*
Manuscript ID:	zaac.201000017.R1
Wiley - Manuscript type:	Article
Date Submitted by the Author:	19-Feb-2010
Complete List of Authors:	Weitzer, Franz; Universität Wien, Innovative Materials Group Naka, Masaaki; Osaka University, Joining and Welding Research Institute Krendelsberger, Natalya; CEST- Center of Electrochemical Surface Technology Stein, Frank; MPI f. Eisenforschung GmbH He, Cuiyun; MPI f. Eisenforschung GmbH Du, Yong; Central South University, State Key Lab for Powder Metallurgy schuster, julius; Universität Wien, Innovative Materials Group
Keywords:	Ni-Si-Ti, ternary system, constitution, phase equilibria, ternary phases

19.2.10

The Ternary System Nickel-Silicon-Titanium Revisited

Franz Weitzer [a], Masaaki Naka [b], Nataliya Krendelsberger [a,c], Frank Stein [d], Cuiyun He [d,e], Yong Du [a,e], and Julius C. Schuster *[a]

Dedicated to Professor Rüdiger Kniep on the Occasion of his 65th Birthday

Keywords: Ni-Si-Ti; ternary system; constitution; phase equilibria; ternary phases;

* Prof. Dr. J.C. Schuster, Fax: +431-4277-9524, eMail: julius.schuster@univie.ac.at
[a] Innovative Materials Group, Universität Wien, Währinger Str. 42, 1090 Wien, Austria
[b] Joining and Welding Research Institute, Osaka University, 11-1 Mihogaoka, Ibaraki 567, Osaka, Japan
[c] CEST-Center of Electrochemical Surface Technology, Viktor Kaplan Str.2, 2700 Wr. Neustadt, Austria
[d] Max-Planck-Institut f. Eisenforschung GmbH, Max-Planck-Str.1, D-40237 Düsseldorf, Germany
[e] State Key Lab for Powder Metallurgy, Central South University, 410083 Changsha, Hunan, P.R.China

Abstract. The constitution of the ternary system Ni-Si-Ti is investigated over the entire composition range using x-ray diffraction (XRD), energy dispersive x-ray spectroscopy (EDS), differential thermal analysis (DTA) and metallography. The solid state phase equilibria are determined for 900 °C. Eight ternary phases are found to be stable. The crystal structures for the phases τ_1NiSiTi, $\tau_2Ni_4Si_7Ti_4$, $\tau_3Ni_{40}Si_{31}Ti_{13}$, $\tau_4Ni_{17}Si_7Ti_6$ and $\tau_5Ni_3SiTi_2$ are corroborated. For the remaining phases the compositions are determined as $Ni_6Si_{41}Ti_{53}$ (τ_6), $Ni_{16}Si_{42}Ti_{42}$(τ_7), and $Ni_{12}Si_{45}Ti_{43}$ (τ_8). The reaction scheme linking the solid state equilibria with the liquidus surface is amended to account for these newly observed phases . The discrepancies between previous experimental conclusions and modeling results are addressed. The liquidus surface is dominated by the primary crystallisation field of τ_1NiSiTi, the only congruently melting phase.

Introduction

In a previous presentation on the system Ni-Si-Ti a liquidus projection derived from experimental data was shown [1]. In the course of that work large areas of the isothermal section at 900 °C were determined, though several tie lines were established only tentatively. Based on these data a thermodynamic description of the entire system was derived by Du et al. [2]. The overall agreement between experiment and model was reasonable but the thermodynamic description deviated in several details from the conclusions derived from the experimental data set. In order to resolve these issues the present study was undertaken. As a first step a brief account on the equilibria observed at 900 °C was presented already [3]. The present paper gives a full documentation of the results for this temperature as well as for the reaction scheme regarding the issues of disagreement between the conclusions from the previous, less complete experimental data set and the thermodynamic modeling.

A comprehensive and critical review of the literature data of the Ni-Si-Ti ternary system is given in [2]. The binary systems used for the present study are based on [4] but are supplemented with

regard to several invariant temperatures as accepted in previous studies [5] (binary Ni-Si), [6] (binary Ni-Ti), and [7,8] (binary Ti-Si).

Experimental

In addition to the about 50 ternary samples prepared in the previous study 20 ternary Ni-Si-Ti samples were newly synthesized by arc melting under high purity argon (from ingots of 99.99 wt.% pure Ni, Si and Ti; all supplied by Johnson Matthey Alfa Products, Karlsruhe, Germany) followed by heat treatment in evacuated quartz tubes at temperatures of 900, 1000 and 1100 °C for up to 1 month. All samples were quenched from the annealing temperature by dropping the quartz tube in cold water. Phase identification was done by X-ray powder diffraction (XRD) using image foil equipped Guinier type chambers (model 670, Huber Diffraktionstechnik, Rimsting, Germany), Cu-Kα_1 radiation, 99.9999 wt.% pure Ge as internal standard), and for data handling and treatment the software packages CSD [9] and STRUKTUR [10]. Phase compositions were determined by energy dispersive spectroscopy (EDS) in a scanning electron microscope (model XL-30-ESEM-FEG, Philips, Einhoven, Netherlands) equipped with EDAX© microanalysis system "Genesis" (S-UTW-Si-(Li)-detector type saphire) and FEI software. Thermal analysis (DTA) was carried out in alumina crucibles under a stream of 99.999 wt.% pure Ar between room temperature and 1500 °C with a heating and cooling rate of 5 K/min using a DTA apparatus (model 701L, from Bähr Thermoanalyse GmbH, Hüllhorst, Germany). The temperature was measured with Pt-Pt/Rh thermocouples calibrated to the melting temperatures of Al (660.3 °C), Ag (961.8 °C), Au (1064.2 °C), Si (1413.8 °C), and Ni (1455.2 °C). The DTA signals read from the heating curves were used. For selected alloys DTA measurements were made up to 1650 °C using a SETSYS-18 DTA from Setaram, France.

Results and discussion

Isothermal section at 900°C and all-solid-state reactions

At 900 °C eight ternary phases are found to be stable. For the phases τ_1 to τ_5 the crystal structures are known (Table 1). XRD and EDS data consistently indicate, that only τ_5-Ni_3SiTi_2 has a noticeable homogeneity range. The other ternary phases are line compounds having very narrow homogeneity ranges centering at their crystallographically nominal compositions (τ_1 to τ_4) or at the EDS-determined compositions $Ni_6Si_{41}Ti_{53}$ (τ_6), $Ni_{16}Si_{42}Ti_{42}$ (τ_7) and $Ni_{12}Si_{45}Ti_{43}$ (τ_8). Fig. 1 shows the tie lines determined. This isothermal section establishes phase equilibria in four different composition regions, where our previous data [1] (reproduced in [2]) were only tentative:

Phase equilibria between binary titanium silicides and τ_1-NiSiTi and/or τ_2-$Ni_4Si_7Ti_4$. For this composition region the literature data are quite controversial proposing a tie line TiSi + τ_1 for 750 °C [15], a tie line Ti_5Si_3 + τ_2 for 1000 °C [16], or the occurrence of a ternary phase $Ni_1Si_4Ti_4$ coexisting with τ_1, τ_2, TiSi and Ti_5Si_4 (but not with Ti_5Si_3) at 1100 °C [17]. Because these reports make it apparent, that equilibrium is difficult to achieve within the quadrangle τ_1 + τ_2 + TiSi + Ti_5Si_3, we not only investigated samples annealed at 900 °C but also samples

annealed at 1000 °C (Table 2). Three ternary phases are identified by EDS and XRD: τ_6 at the composition $Ni_6Si_{41}Ti_{53}$, τ_7 at the composition $Ni_{16}Si_{42}Ti_{42}$, and τ_8 at the composition $Ni_{12}Si_{45}Ti_{43}$. The XRD patterns of all three phases are similar, but extremely complicated. The XRD pattern of the last phase (τ_8) indicates this phase to be isostructural to the phase τ_9 of the system Fe-Si-Ti [8]. Furthermore, τ_8 corresponds to the phase $Ni_1Si_4Ti_4$ reported by Hu et al. [17]. The tie lines observed in the present study corroborate for 900 °C all tie lines found for this phase at 1100 °C [17] . We find, however, in addition the phase τ_6 within the phase triangle τ_8 + Ti_5Si_4 + Ti_5Si_3 and the phase τ_7 within the phase triangle τ_1 + Ti_5Si_4 + τ_8 (Fig. 1).

Occurrence of Ni_3Si_2 at 900 °C. No θNi_2Si is observed within the composition range δNi_2Si – NiSi – $\tau_3Ni_{40}Si_{31}Ti_{13}$ in samples which were quenched from 900 °C to ambient. Instead Ni_3Si_2 is found (Table 2). DTA measurements, however, made clear that the absence of θNi_2Si as well as the appearance of Ni_3Si_2 in these samples at room temperature does not represent equilibrium, but rather is due to insufficient quenching rates achieved by the experimental procedure applied. Thus, samples #19 and #20 consisted after quenching from the annealing temperature of δNi_2Si, Ni_3Si_2, and τ_3. Both show upon heating a DTA signal at 822±1 °C (onset), which coincides with the temperature of 821±2 °C reported for the formation of θNi_2Si from δNi_2Si + Ni_3Si_2 in binary Ni-Si [18,19]. Furthermore, the DTA peak at 862±1 °C in samples #17 and #18 (consisting of NiSi, Ni_3Si_2, and τ_3 after quenching from the annealing temperature) has to be associated with the decomposition of Ni_3Si_2 into θNi_2Si + NiSi, which is reported to occur in the binary at 860±2 °C [18] or 865 °C [19], respectively. Upon cooling both DTA peaks occur, too. Thus, at 900 °C no Ni_3Si_2 exists in the phase field θNi_2Si – NiSi – τ_3 (Fig. 1).

Homogeneity range of $Ni_3(Si,Ti)$. The extensive substitution of Si by Ti in Ni_3Si [20] is corroborated. The lattice parameters increase with the Ti-content monotonously from a = 0.3504 nm for binary Ni_3Si (Cu_3Au-type, $L1_2$, *Pm*-3*m*, cP4[21]) to a = 0.35374(6) nm for $Ni_{73.9}Si_{20.0}Ti_{6.1}$ in sample #27, and to a = 0.35644(7) nm for $Ni_{75.1}Si_{12.7}Ti_{12.2}$ in sample #29 (Table 2). Thus, about half of the Si atoms are replaced by Ti. The latter phase is in equilibrium with Ni_3Ti and $\tau_4Ni_{17}Si_7Ti_6$ (Fig. 2a). For these two phases the compositions measured do not significantly deviate from the nominal compositions.

Coexistence of τ_1NiSiTi and NiTi. Previous literature consistently reports a tie line between Ti_5Si_3 and $\tau_5Ni_3SiTi_2$ (for 750 °C [15], for 1000 °C [16], for 1100 °C [17]) as well as the occurrence of a ternary phase with the approximate composition Ni_5SiTi_6 [17,18]. Only Xu and Jin [22] reported a sample equilibrated at 900 °C in which NiTi coexists with τ_1NiSiTi. However, Ni_3Ti was observed as third phase in this sample, which indicates that this sample was not in equilibrium. Previous results from our own samples were not conclusive either: XRD data from powdered samples did not allow to identify NiTi, because this phase "disappears" during pulverization due to its ductility. The EDS data on the other hand were "corrupted" due to the very small particle size in these samples (eg. in Table 2 the composition found for Ti_5Si_3 in sample #37).

In the present investigation supplementary XRD using polished sample plates was conducted for a few samples in a conventional diffractometer. The XRD patterns obtained (Fig. 3) allowed the

clear identification of NiTi having at room temperature monoclinic B19'-type crystal structure (spacegroup $P2_1/m$), which forms from the cubic B2-type structure by a martensitic transformation upon quenching the phase to room temperature [22]. Furthermore extended annealing produced sufficient grain growth for reliable EDS analysis (Table 2). Thus the existence of the three-phase fields NiTi + τ_1 + Ti_5Si_3 (sample #40, Fig. 2b) as well as NiTi + τ_1 + τ_5 at 900 °C is unambigously observed. No ternary phase with a composition Ni_5SiTi_6 is found. Small DTA signals at 1066±1 °C (samples #36 and #37) indicate an all solid state reaction, however. To identify the origin of these DTA signals annealing experiments at 1100 °C were conducted. The results of these experiments show, that the tie line NiTi + τ_1 changes at 1066 °C to Ti_5Si_3 + τ_5 upon heating (Table 2, samples #37 and #39).

Reaction scheme involving the liquid phase and liquidus projection

The reaction scheme showing all invariant equilibria involving the liquid phase as well as the all-solid-state reactions documented in the previous section is given in Figs. 4a-c. It is derived from (1) the above described new results regarding the isothermal section at 900 °C prompting in part a reinterpretation of the DTA signals, as well as (2) from DTA measurements of new alloys specifically designed to probe all modeling results by Du et al. [2] disagreeing with our previous conclusions which were based purely on experimental evidence [1]. The present results clarify the following issues:

Formation of the ternary phases τ_2, τ_6, τ_7, and τ_8. Due to the lack of data our first assumption about invariant reactions involving the liquid phase in the Si-rich composition region was quite tentative [1]. None of the high melting phases τ_6, τ_7, or τ_8 was considered. The formation of τ_2 was assumed to be by peritectic reaction from L + τ_1 + TiSi. The latter assumption was modified already by [2] to p_{max}: L + τ_1 = τ_2. This is corroborated in the present study by microstructure evidence of the as cast samples showing primary τ_1 surrounded by seams of τ_2. Combining microstructure and DTA-data (Table 2) shows, that the phases τ_6, τ_7, and τ_8 form all from the melt by peritectic reactions involving the phase Ti_5Si_4: P_1: L + Ti_5Si_3 + Ti_5Si_4 $\Rightarrow$ τ_6 at a temperature above 1600 °C; P_2: L + Ti_5Si_4 + τ_1 $\Rightarrow$ τ_7 at 1545 °C; and P_3: L + Ti_5Si_4 + τ_7 $\Rightarrow$ τ_8 at 1497 °C (Fig. 4a). The fields of primary crystallisation of each of these phases are very limited (Fig. 5).

Formation of the ternary phase τ_3. From the set of experimental data a peritectic reaction L + τ_1 + τ_4 $\Rightarrow$ τ_3 was concluded [1], but modeling asked for a maximum in the temperature for the monovariant equilibrium L + τ_1 = τ_3 [2]. The DTA for samples #23 as well as #24 (consisting after equilibration only of the phases τ_1 + τ_3) clearly shows that the lowest onset temperature is 1271±1 °C, which is higher than the temperatures found in samples consisting either of τ_1 + τ_3 + τ_2 (1170 °C for sample #16) or τ_1 + τ_3 + τ_4 (1259 °C for sample #22). Thus, the model predicted formation of τ_3 in a peritectic maximum p_{max4}: L + τ_1 $\Rightarrow$ τ_3 is experimentally corroborated (Figs. 4a and b).

Temperature maximum in the monovariant equilibrium L = θNi_2Si + τ_3. DTA of samples #17-21 shows the liquidus temperatures to increase with decreasing silicon content (Table 2). Although

these samples contain after equilibration at 900 °C δNi_2Si and/or εNi_3Si_2 rather than θNi_2Si, they all undergo upon heating up solid state transformations resulting in the presence of $\theta Ni_2Si + \tau_3$ (besides additional NiSi samples #17and #18 and τ_4 in sample #21, respectively). Thus, the temperature of the monovariant equilibrium $L + \theta Ni_2Si + \tau_3$ increases from 950 °C (samples #17 and #18, E_4: $L = NiSi + \theta Ni_2Si + \tau_3$) to 1134 °C (sample #21, U_{15}: $L + \tau_4 = \theta Ni_2Si + \tau_3$). As the intermediate samples #19 and #20 melt at 1092 °C and 1118 °C respectively, no evidence for a maximum is observed. Thus, in this point the model prediction cannot be confirmed.

Existence of a ternary eutectic $L = Ni_{31}Si_{12} + Ni_3Si + \tau_4$. The corroboration and thus acceptance of the literature data [20] concerning the extensive substitution of Si by Ti in Ni_3Si (Fig. 1) leads to the conclusion, that the monovariant equilibrium $L + Ni_{31}Si_{12} + Ni_3Si$ is crossing this extended $Ni_3(Si,Ti)$ single phase region. This crossing involves the change from the binary peritectic reaction $L + Ni_{31}Si_{12} \Rightarrow Ni_3Si$ to an eutectic reaction $L \Rightarrow Ni_{31}Si_{12} + Ni_3Si$ in the ternary system at about 4-5 at. % Ti. With this finding a ternary eutectic E_2: $L = Ni_{31}Si_{12} + Ni_3Si + \tau_4$ as predicted by modeling [2] becomes the most parsimonious interpretation of the DTA data in the Ni-rich corner (Fig. 4b).

Formation of the ternary phase τ_5. Sample #41 was designed to test whether a maximum exist in the monovariant equilibrium $L + \tau_1 = \tau_5$ as predicted by modeling [2]. DTA clearly shows that the melting temperature (1412 °C) in this sample (consisting only of the two phases τ_1 and τ_5) is higher than the respective onset temperatures in samples consisting either of $\tau_1 + \tau_5 + \tau_4$ (1395 °C for sample #33) or $\tau_1 + \tau_5 + Ti_5Si_3$ (1196 °C for sample #39). Thus, the model predicted formation of τ_5 in a peritectic maximum p_{max3}: $L + \tau_1 \Rightarrow \tau_5$ is experimentally corroborated (Fig. 4c).

Temperature maximum in the monovariant equilibrium $L = Ni_3Ti + \tau_5$. The model predicted occurrence of such a maximum in $L = Ni_3Ti + \tau_5$ requires the existence of a ternary eutectic $L = Ni_3Ti + \tau_5 + \tau_4$. Already Hao et al. [24] were searching for such a ternary eutectic. One of their samples had a composition within the phase triangle $Ni_3Ti + \tau_5 + \tau_4$, but no ternary eutectic was observed. Thus the model predicted existence of such a ternary eutectic is not supported by experimental data.

Temperature maximum in the monovariant equilibrium $L = NiTi + \tau_5$. Sample #35 was designed to test whether a maximum exist in the monovariant equilibrium $L = NiTi + \tau_5$ as predicted by modeling [2]. DTA clearly shows that the melting temperature (1162 °C) in this sample (consisting only of the two phases NiTi and τ_5) is higher than the respective onset temperatures in samples consisting either of $Ni_3Ti + NiTi + \tau_5$ (1068 °C for sample #31) or $NiTi + \tau_5 + Ti_5Si_3$ (1137 °C for sample #37). Thus, the model prediction for the existence of e_{max4}: $L = NiTi + \tau_5$ is corroborated by experiments. This temperature maximum in the monovariant equilibrium $L + NiTi + \tau_5$ implies the existence of an additional ternary eutectic $L = NiTi + \tau_5 + Ti_5Si_3$ [2]. The melting temperature for this eutectic (E_1 in Fig. 4c) is determined as 1137±1 °C in samples where τ_5 was not present at the beginning of the DTA run, but formed only during heating by the reaction $\tau_1 + NiTi \Rightarrow \tau_5 + Ti_5Si_3$ (samples #37, 39, and 40). In samples with preexisting τ_5 the temperature observed was about 5K higher (sample #36), but still below e_{max5}: $L = NiTi + Ti_5Si_3$ observed at 1146 °C in sample #42.

Fig. 3 shows the liquidus projection derived from the reaction scheme (Figs. 4a-c) combined with the metallographic observations of the primary phases crystallizing (Table 3). The liquidus surface is dominated by τ_1, the only ternary phase with a congruent melting point. The wide area of primary crystallisation of τ_1 together with its incongruently melting "satelite phases" τ_2, τ_3, τ_4, and τ_5 is confined by a loop of connecting eutectic troughs. On the Si-rich side of the saddle point e_{max1} (between τ_1 and Ti_5Si_3) this trough descends monotonously from T > 1600 °C through several peritectics (formation of τ_6 and τ_7) and transition reactions and ends in the ternary eutectic E_5: L = τ_2 + $NiSi_2$ + NiSi at 935 °C. On the Ti-rich side of the saddle point e_{max1} the eutectic ends in the ternary eutectic E_1: L = τ_5 + NiTi + Ti_5Si_3 at 1137 °C. Along the Ni-rich side the eutectic trough is separated from τ_1 by the primary crystallisation fields of τ_2, τ_3, τ_4, and τ_5, which all form in peritectic maxima from L + τ_1. The eutectic trough itself crosses along the Ni-rich side (connecting E_5 and E_1) four maxima (e_{max6} between τ_3 and NiSi; e_{max3} between τ_4 and θNi_2Si; e_{max2} between τ_4 and Ni_3Ti; and e_{max4} between τ_5 and NiTi) separated by three minima (E_4: L = τ_3 + NiSi + θNi_2Si; E_2: L = τ_4 + $Ni_{31}Si_{12}$ + Ni_3Si; and E_3: L = τ_5 + Ni_3Ti + NiTi). The compositions of the latter two ternary eutectics were determined by EDS area scans as $Ni_{70}Si_{20.5}Ti_{9.5}$ (for E_2) and $Ni_{60.5}Si_4Ti_{35.5}$ (for E_3). Finally, the Ti-rich ternary eutectic E_6: L = Ti_5Si_3 + $NiTi_2$ + β(Ti) is found to have the composition $Ni_{19}Si_7Ti_{74}$.

Conclusions

The isothermal section at 900 °C for Ni-Si-Ti over the entire composition range is established. Eight ternary phases are stable at this temperature. Except for τ_5 all these ternary phases have very narrow homogeneity ranges. The crystal structures for the phases τ_1 to τ_5 are all corroborated. For the phases τ_6 to τ_8 the compositions were determinded. The phase τ_8 corresponds to the phase $NiSi_4Ti_4$ reported by Hu [17]. No phase Ni_5SiTi_6 is found. Based on these results and the interpretation of DTA and SEM/EDS data a reaction scheme linking the equilibria observed at 900 °C with the liquidus surface is derived. All ternary phases are stable up to the melt. Only τ_1 melts congruently. The phases τ_2, τ_3, τ_4 and τ_5 all form in peritectic maxima from L + τ_1. The phases τ_6, τ_7 and τ_8 form in peritectic reactions from L + Ti_5Si_4 + a third phase. Six ternary eutectics occur. A liquidus projection is derived by linking the reaction scheme with determinations of the primary phase crystallising and of the compositions determined by EDS for several of the ternary eutectics.

Acknowledgements

This work was in part financially supported by the Austrian Science Foundation (grants P12843 and P12113) and the Scientific-Technological Cooperation between Austria and the P.R. of China (ÖAD grant WTZ VII.B.9).

References

[1] J. C. Schuster, H. Takase, I. Nakade, and M. Naka, **2002,** in M. Naka (Ed.): *Designing of Interfacial Structures in Advanced Materials and their Joints,* JWRI, Osaka Univ., Osaka, Japan, p 443ff
[2] Y. Du, C. He, J. C. Schuster, S. H. Liu, H. H. Xu, *Int. J. Mater. Res*. **2006**, *97,* 543.
[3] F. Weitzer, N. Krendelsberger, J. C. Schuster, *Adv. Appl. Plasma Sci*. **2009,** *7*, 270.
[4] T. B. Massalski (ed.), **1990,** *Binary Alloy Phase Diagrams*, 2nd ed., ASM Intl., Mater. Park, OH., USA.
[5] S. Ackerbauer, N. Krendelsberger, F. Weitzer, K. Hiebl, J. C. Schuster, *Intermetallics* **2009**, *17*, 414.
[6] J. C. Schuster, Z. Pan, S. H. Liu, F. Weitzer, Y. Du, *Intermetallics* **2007**, *15*, 1257.
[7] S. H. Liu, F. Weitzer, J. C. Schuster, N. Krendelsberger, Y. Du, *Intl. J. Mater. Res*. **2008,** *99*, 705.
[8] F. Weitzer, J. C. Schuster, M. Naka, F. Stein, M.Palm, *Intermetallics* **2008**, *16*, 273.
[9] L. G. Akselrud, Y. N. Grin, P. Y. Zavalij, V. K. Pecharsky, V. S. Fundamensky, *Coll.Abstr. 12th Eur. Crystallogr. Meeting, Moskow, 1989* in: *Izv. Akad. Nauk SSSR*, *Moskov*, **1989,** *3*, 155.
[10] W. Wacha, master thesis, *Vienna Inst. Technology, Vienna, Austria*, **1989.**
[11] C. B. Shoemaker, D. P. Shoemaker, *Acta Crystallogr*. **1965**, *18*, 900.
[12] W. Jeitschko, A. G. Jordan, P. A. Beck, *Trans. Met. Soc. AIME* **1969,** *245*, 335.
[13] A. Grytsiv, X. Q. Chen, P. Rogl, R. Podloucky, H. Schmidt, G. Giester, V. Pomjakushin, *J. Solid State Chem.* **2007**, *180***,** 733.
[14] D. I. Bardos, K. P. Gupta, P. A. Beck, *Trans. Met. Soc. AIME* **1961**, *221***,** 1087.
[15] V. Ya. Markiv, E. I. Gladyshevskii, P. I. Kripyakevich, T. I. Fedoruk, *Izv. Akad. Nauk SSSR, Neorgan. Mater*. **1966**, *2*, 1317.
[16] J. H. Westbrook, R. K. DiCerbo, A. J. Peat, **1958**, *GE Research Report 58-RL-2117*, p1ff.
[17] X. Hu, G. Chen, C. Ion, K. Ni, *J. Phase Equilibria* **1999**, *20*, 508.
[18] Y. Du, J. C. Schuster, *Metall. Trans*. *A* **1999**, *30A*, 2409.
[19] K. Richter, K. Chandrasekaran, H. Ipser, *Intermetallics* **2004**, *12*, 545.
[20] K. Takasugi, D. Shindo, O. Izumi, M. Hirabayashi, *Acta Met. Mater*. **1990**, *38*, 739.
[21] P. Villars, L. D.Calvert, **1985**, *Pearson's Handbook of Crystallographic Data for Intermetallic Phases*, ASM, Metals Park, OH, USA
[22] H. H. Xu, Z. P. Jin, *Trans. Nonferrous Met. Soc. China* **1998**, *8*, 1
[23] G. R. Purdy, J. G. Parr, *Trans. Met. Soc. AIME* **1961**, *221,* 636
[24] G. Haour, F. Mollard, B. Lux, I. G. Wright, *Z. Metallkd*. **1978**, *69*, 149

Figure Captions

Fig. 1: Solid state phase equilibria at 900 °C

Fig. 2a: SEM micrograph of sample #29 ($Ni_{69.9}Si_{9.7}Ti_{20.4}$) equilibrated at 900 °C showing $Ni_3(Si,Ti)$ (grey phase) coexisting with Ni_3Ti (bright phase) and τ_4 (dark phase)
Fig. 2b:SEM micrograph of sample #40 ($Ni_{27.6}Si_{24.8}Ti_{47.6}$) equilibrated at 900 °C showing coexistence of the phases NiTi (bright phase) + τ_1 (grey phase) + Ti_5Si_3 (dark phase)

Fig. 3: XRD powder pattern (Cu-Kα_1 radiation) of a polished alloy plate (sample #38, $Ni_{44.8}Si_{10.1}Ti_{45.1}$ equilibrated at and quenched from 900°C) showing NiTi (B19'-type structure) coexisting with τ_1NiSiTi

Fig. 4: Reaction scheme connecting the liquid phase with the solid state equilibria
a) in the Si-rich region
b) in the Ni-rich region

c) in the Ti-rich region
Temperatures are given in °C

Fig. 5: Liquidus projection of the system Ni-Si-Ti

Table 1: Ternary Ni-Si-Ti phases: crystal structures, lattice parameters and compositions

phase	structure type Pearson code space group	Lattice parameters (nm) literature	observed (Vmin)	observed (Vmax)	ratio V_{max}/V_{min}	composition at. % Ni/ Si/ Ti
τ_1NiSiTi, (E-phase)	Co_2Si-type oP12 *Pnma* (#62)	a = 0.6148 b = 0.3670 c = 0.7017 ref. [11]	a = 0.6144(3) b = 0.3668(1) c = 0.7011(1)	a = 0.6145(1) b = 0.3687(1) c = 0.7021(2)	1.007	nominal 33.3/33.3/33.3 obs. at 33±2/33±4/34±2
$\tau_2Ni_4Si_7Ti_4$ ($NiSi_2Ti$, V-phase)	$Co_4Ge_7Zr_4$-type tI60 *I4/mmm* (#139)	a = 1.2575 c = 0.4945 ref. [12]	a = 1.25452(8) c = 0.49354(5)	a = 1.2574(1) c = 0.4942(1)	1.004	nominal 26.7/46.7/26.7 obs. at 27±1/44±2/29±1
$\tau_3Ni_{40}Si_{31}Ti_{13}$ (Ni_4Si_3Ti, G"-phase)	$Pd_{40}Si_{31}Y_{13}$-type hP168 *P6/mmm* (#191)	a = 1.7173 c = 0.7861 ref. [1]	a = 1.7162(2) c = 0.7879(5)	a = 1.7217(2) c = 0.7851(3)	1.006	nominal 47.6/36.9/15.5 obs. at 47.0/38.5/14.5 in ref. [1]
$\tau_4Ni_{17}Si_7Ti_6$ (G-phase, T-phase)	(partially) filled $Mn_{23}Th_6$ –type cF120 *Fm*-3*m* (#225)	a = 1.12595(2) ref. [13]	a = 1.1222(1)	a = 1.12557(5)	1.003	nominal 57.7/23.3/20.0 obs. at 57±1/24±1/19±1
$\tau_5Ni_3SiTi_2$ (G'-phase, λ-phase)	$MgZn_2$-type hP12, C14 $P6_3/mmc$ (#194)	a = 0.479 c = 0.755 ref. [14]	a = 0.47806(6) c = 0.7668(2)	a = 0.48135(2) c = 0.77111(4)	1.020	nominal 50/16.7/33.3 obs. at 51/17/32 (coex. with Ni_3Ti + NiTi) 43/22/35 (coex. with NiTi + τ_1)
τ_6						obs. at 6/41/53
τ_7						obs. at 16/41-42/42-43
τ_8 ($NiSi_4Ti_4$, H-phase)		ref. [17]				"nominal" 11.1/44.4/44.4 obs. at 12±1/45/43±1
Ni_5SiTi_6 (F-phase, X-phase)		ref.[17, 18]				"nominal" 41.7/8.3/50.0 not observed

Table2: Results of EDX, XRD, and thermal characterization of representative samples

	composition (at %)					EDS results (at %)			
alloy #	Ni	Si	Ti	heat treatment	phases identified by XRD	Ni	Si	Ti	DTA signals (°C) on heating at a rate of 5 K/min
1	3	42	55	1000 °C, 4w	Ti_5Si_4 Ti_5Si_3 τ_6	0.3 0.2 5.2	45.3 39.1 41.1	54.4 60.7 53.7	no signal below 1600 °C
2	8.4	36.2	55.4	900 °C, 6d	Ti_5Si_3 τ_1 τ_6	1.5 33.9 6.7	36.2 32.3 38.1	62.3 33.8 55.2	no signal below 1600 °C
3	20	37	43	1000 °C, 4w	Ti_5Si_3 τ_1 τ_6	0.9 31.3 6.3	39.2 35.6 41.2	59.9 33.1 52.5	(1597) U_1 1605 ?
4	6.5	40.6	52.9	1000 °C, 4w	τ_1 τ_6 Ti_5Si_4	31.7 5.8 1.0	34.8 40.8 44.0	33.5 53.4 55.0	1545 P_2 1578 U_2 1595 U_1
5	15	42.5	42.5	1000 °C, 4w	Ti_5Si_4 τ_7 τ_8				1497 P_3 1545 P_2
6	10.0	43.1	46.9	1000 °C, 2w	Ti_5Si_4 τ_7 τ_8	0.5 16.1 11.9	43.5 40.9 44.2	56.0 43.0 43.9	1495 P_3
7	5	45	50	1000 °C, 4w	TiSi Ti_5Si_4 τ_8	1.0 0.3 12.0	49.5 44.0 44.4	49.5 55.7 43.6	1452 U_4
8	24.8	45.4	29.8	900 °C, 6d	τ_1 τ_2 τ_8				1353 U_6 1476 U_3
9	25.1	40.0	34.8	900 °C, 6d	τ_1 τ_2 τ_8	31.5 27.0 12.0	35.6 44.5 45.5	32.9 28.5 42.5	1353 U_6
10	9	46	45	1000 °C, 4w	TiSi τ_2 τ_8	0.4 26.6 11.7	50.4 42.7 45.0	49.2 30.7 43.3	(1070) U_{18} 1270 U_8 (1320) U_7
11	10.0	55.3	34.7	900 °C, 6d	$TiSi_2$ TiSi τ_2				1269 U_8 1321 U_7
12	10.0	69.9	20.1	900 °C, 6d	(Si) $TiSi_2$ τ_2				1067 U_{18} 1222 liqu.
13	20.0	69.8	10.2	900 °C, 6d	(Si) $NiSi_2$ τ_2				945 U_{21} 1068 U_{18} 1188 liqu.

14	35.2	55.1	9.6	900 °C, 6d	$NiSi_2$ NiSi τ_2				935 E_5 952 U_{21}
15	44.9	45.3	9.8	900 °C, 6d	NiSi τ_2 τ_3				954 U_{20} 1206 liqu. 1229 liqu.
16	34.9	39.7	25.4	900 °C, 6d	τ_1 τ_2 τ_3				1170 U_{14}
17	50	45	5	900 °C, 8d	NiSi Ni_3Si_2 τ_3				862 bin. Ni-Si 951 E_4
18	51.4	41.7	6.8	900 °C, 6d	NiSi Ni_3Si_2 τ_3				(863) bin. Ni-Si 950 E_4 1218 liqu. 1436 liqu.
19	56.2	37.0	6.8	900 °C, 6d	Ni_3Si_2 δNi_2Si τ_3				822 bin. Ni-Si 1092 $E_4 \rightarrow U_{15}$ 1173 liqu. 1245 liqu.
20	56.5	36.5	7.0	900 °C, 4w	Ni_3Si_2 Ni_2Si τ_3				(820) bin. Ni-Si 1118 $E_4 \rightarrow U_{15}$ 1179 liqu. 1240 liqu.
21	56.6	33.4	10.0	900 °C, 6d	δNi_2Si τ_3 τ_4				1134 U_{15} 1184 e_{max3}
22	44.7	32.1	23.2	900 °C, 6d	τ_1 τ_3 τ_4				1259 U_9 1446 liqu.
23	47.6	36.9	15.5	900 °C, 6d	τ_1 τ_3				1269 p_{max4}
24	42	35.5	22.5	900 °C, 4w	τ_1 τ_3				1273 p_{max4}
25	62.3	27.5	10.2	900 °C, 6d	δNi_2Si $Ni_{31}Si_{12}$ τ_4				1176 U_{13} 1184 e_{max3}
26	70	25	5	900 °C, 8d	$Ni_{31}Si_{12}$ Ni_3Si τ_4				1095 E_2 1155 liqu. 1208 liqu.
27	69.2	20.4	10.4	900 °C, 6d	Ni_3Si τ_4	73.9 57.3	20.0 25.3	6.1 17.4	1093 E_2 1290 liqu.
28	75	12.5	12.5	900 °C, 4w	Ni_3Si τ_4	75.2 59.4	13.2 23.5	11.6 17.1	1106 $E_2 \rightarrow U_{17}$ 1163 liqu.
29	69.9	9.7	20.4	900 °C, 6d	Ni_3Si Ni_3Ti τ_4	75.1 74.9 57.6	12.7 1.7 23.7	12.2 23.4 18.7	1119 U_{17} 1198 liqu.
30	70	7	23	900 °C, 8d	Ni_3Ti				1224 e_{max2}

					τ_4				1304 liqu.
31	56.7	8.1	35.2	900 °C, 6d	Ni_3Ti NiTi τ_5	73.7 52.9 49.6	0.8 1.1 17.4	25.5 46.0 33.0	1068 E_3
32	57.7	15.7	26.6	900 °C, 6d	Ni_3Ti τ_4 τ_5				1180 U_{12} 1392 U_5
33	45.0	25.1	29.9	900 °C, 6d	τ_1 τ_4 τ_5				(1395) U_5 1487 p_{max2}
34	47	27	26	900 °C, 2w	τ_1 τ_4				1487 p_{max2}
35	49.5	7.5	43	900 °C, 4w	τ_5 NiTi	46.7 51.6	19.1 1.0	34.2 47.4	1162 e_{max4}
36	45	15	40	900 °C, 4w	τ_1 τ_5 NiTi	32.9 43.3 49.1	33.9 21.5 1.9	33.2 35.3 49.0	(1067) u 1144 E_1
37	40	15	45	900 °C, 4w	τ_1 Ti_5Si_3 NiTi	33.5 13.5 47.4	33.3 30.5 2.9	33.2 56 49.7	(1066) u 1137 E_1
				1100 °C, 2d	τ_5 Ti_5Si_3 NiTi				
38	44.8	10.1	45.1	900 °C, 6d	NiTi τ_1	49.4 34.7	2.0 29.8	48.6 35.5	1140 E_1 1167 liqu.
39	30.1	25.0	44.9	900 °C, 6d	Ti_5Si_3 τ_1 NiTi				1137 E_1 1198 U_{11}
				1100 °C, 2d	Ti_5Si_3 τ_1 τ_5				
40	27.6	24.8	47.6	900 °C, 6d	Ti_5Si_3 τ_1 NiTi	2.0 34.0 49.2	36.7 31.9 2.1	61.3 34.1 48.7	1136 E_1 (1205) U_{11}
41	41.5	25.0	33.5	900 °C, 4w	τ_1 τ_5	33.5 49.4	33.4 18.7	33.1 31.9	1412 p_{max3}
42	36.4	10.5	53.1	900 °C, 4w	Ti_5Si_3 NiTi	6.0 49.4	31.2 1.0	62.8 49.6	1146 e_{max5}
43	16.5	25.7	57.8	900 °C, 6d	Ti_5Si_3 NiTi $NiTi_2$	1.8 49.3 32.0	36.9 1.0 1.8	61.3 49.7 66.2	959 U_{19} 1129 liqu.
44	30.1	9.6	60.3	900 °C, 4w	Ti_5Si_3 Ni Ti_2 NiTi				960 U_{19} 1105 liqu.
45	15.0	16.9	68.1	900 °C, 6d	Ti_5Si_3 $NiTi_2$ α(Ti)				918 E_6
46	7.0	25.3	67.8	900 °C, 6d	Ti_5Si_3				920 E_6

					$NiTi_2$ α(Ti)				

Table 3: Primary phases crystallizing (identified in as cast microstructures by EDS)

sample composition (at. %)			primary phase	additional observations
Ni	Si	Ti		
85.9	3.8	10.3	(Ni)	
76.6	2.6	20.8	Ni_3Ti	+ eu (Ni_3Ti + Ni_3Si) at (73/13.7/13.3)
62.8	4.2	33.0	Ni_3Ti	+ eu (Ni_3Ti + τ_5)
60.4	4.0	35.6	E_3	= eu (Ni_3Ti + τ_5 + NiTi) at (60.5/4.0/35.5)
54.1	3.6	42.3	NiTi	+ (secondary) Ni_3Ti + τ_5
35.0	1.5	63.5	NiTi	+ eu ($NiTi_2$ + β(Ti)) at (21.8/3.6/74.6)
25.0	4.8	70.2	$NiTi_2$	+ E_6 ($NiTi_2$ + Ti_5Si_3 + β(Ti)) at (18.8/6.9/74.3)
14.3	4.0	81.7	β(Ti)	+ eu ($NiTi_2$ + β(Ti)) at (20.9/3.6/75.5)
83.0	11.6	5.4	(Ni)	
71.1	12.7	16.2	Ni_3Ti	+ (secondary) τ_4
66.4	12.2	21.4	τ_4	+ eu (Ni_3Ti + τ_4)
62.3	12.1	25.6	τ_4	+ eu (τ_4 + τ_5) at (60.5/9.3/30.2)
54.8	8.1	37.1	τ_5	+ (secondary) Ni_3Ti
50.6	8.2	41.2	τ_5	+ (secondary) Ti_5Si_3 + NiTi
45.5	11.9	42.6	τ_1	+ eu (τ_1 + Ti_5Si_3) at (35.5/15.5/49)
40.7	10.3	49.0	Ti_5Si_3	+ (secondary) NiTi
62.7	16.0	21.3	τ_4	
59.5	17.7	24.8	τ_4	+ eu (τ_4 + τ_5) at (58.1/13.0/28.9)
50.6	17.4	32.0	τ_1	+ (secondary) τ_5
49.4	18.0	32.6	τ_1	+ (secondary) $Ni_{31}Si_{12}$
41.1	15.9	42.9	τ_1	
75.5	21.4	3.1	$Ni_{31}Si_{12}$	+ E_2 ($Ni_{31}Si_{12}$ + τ_4 + Ni_3Si) at (70/20.5/9.5)
67.9	20.0	12.1	τ_4	+ (secondary) $Ni_{31}Si_{12}$
64.9	20.5	14.6	τ_4	+ eu (θNi_2Si + τ_4) at (65/29.3/5.7)
59.3	19.3	21.4	τ_4	
48.7	21.1	30.2	τ_1	+ (secondary) τ_4
22.2	20.5	57.2	Ti_5Si_3	
59.6	35.4	5.0	θNi_2Si	+ (secondary) NiSi + τ_3
54.1	32.3	13.6	τ_1	
49.6	32.9	17.5	τ_1	+ (secondary) τ_3
45.3	33.5	21.2	τ_1	+ (secondary) τ_2
23.7	35.6	40.7	τ_1	+ (secondary) τ_6
16.0	33.7	50.3	τ_1	+ (secondary) Ti_5Si_3
6.3	30.4	63.3	Ti_5Si_3	+ (secondary) τ_1
45.4	39.9	14.7	τ_2	
42.3	45.7	12.0	τ_2	+ (secondary) NiSi + $NiSi_2$
40.9	38.7	20.4	τ_1	+ (secondary) τ_2 + τ_3
36.6	45.5	17.9	τ_2	+ (secondary) NiSi + $NiSi_2$
30.9	37.1	32.0	τ_1	+ (secondary) τ_2

24.4	43.5	32.1	τ_1	
15.0	42.6	42.4	τ_6	+ (secondary) τ_7
14.5	38.8	46.7	Ti_5Si_3	+ (secondary) $\tau_6 + \tau_7$
18.3	58.2	23.5	τ_2	+ (secondary) NiSi + $NiSi_2$

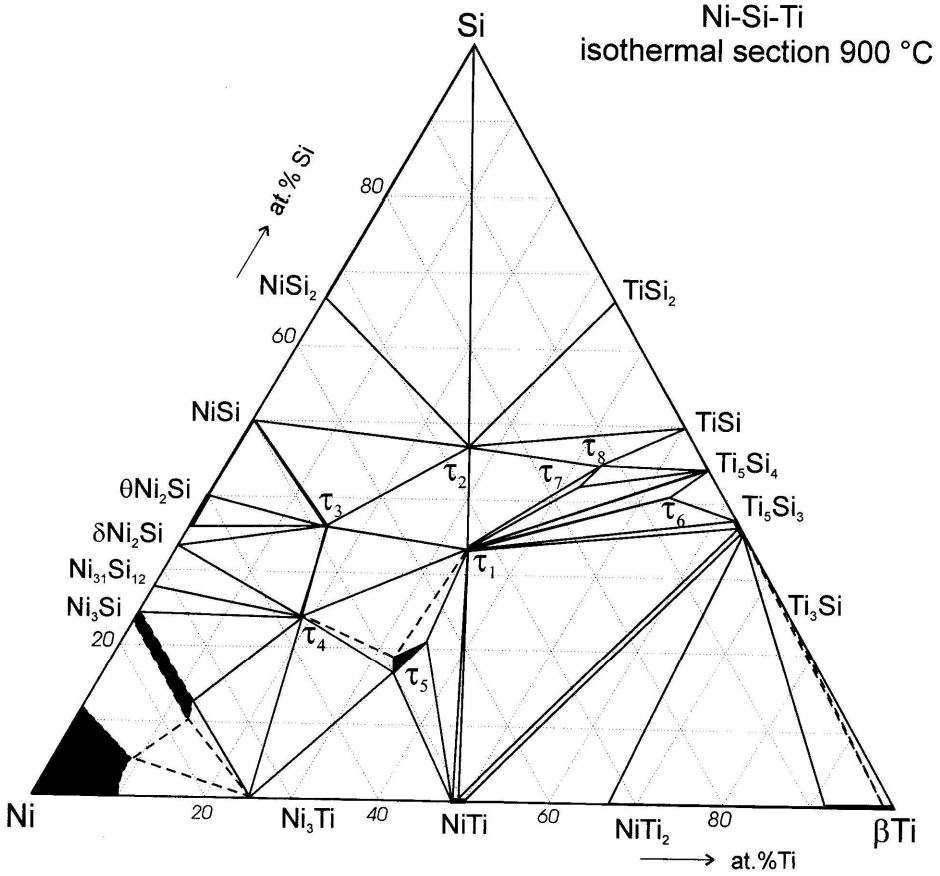

176x162mm (300 x 300 DPI)

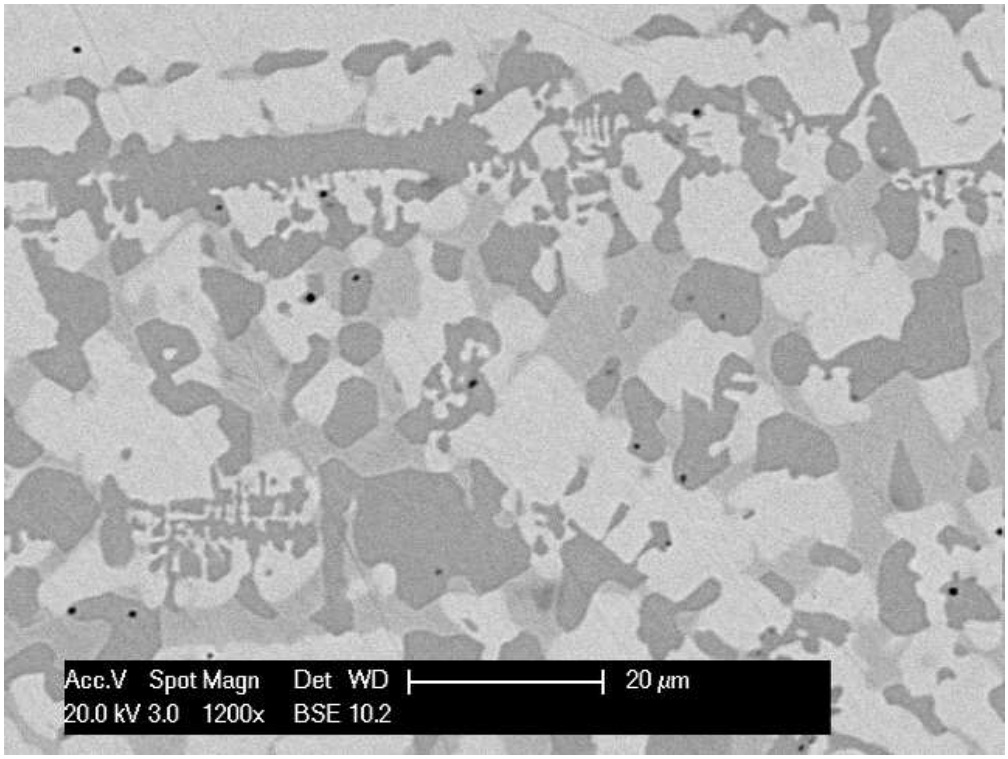

81x61mm (200 x 200 DPI)

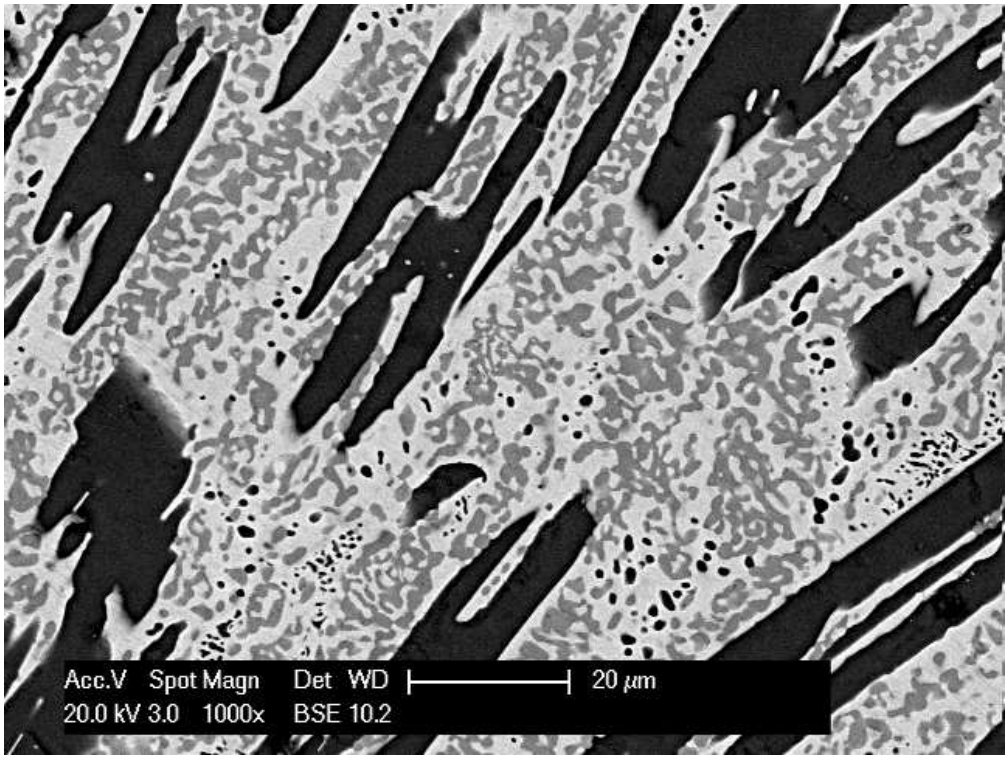

81x61mm (200 x 200 DPI)

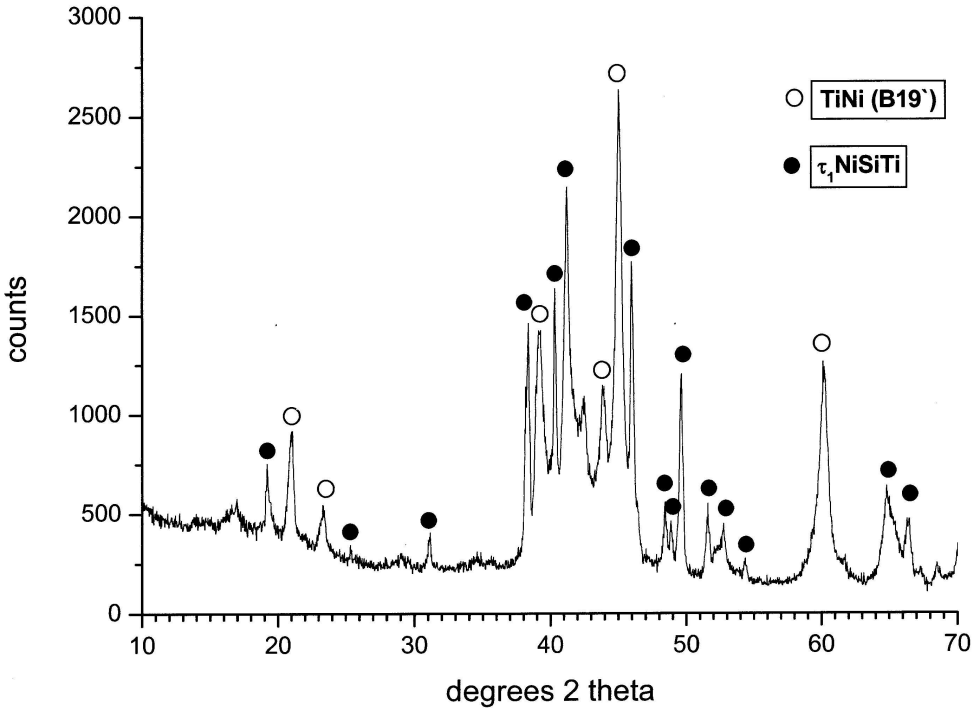
3000
2500
2000
1500
1000
500
0
counts
10
20
30
40
50
60
70
degrees 2 theta
TiNi (B19`)
τ1NiSiTi

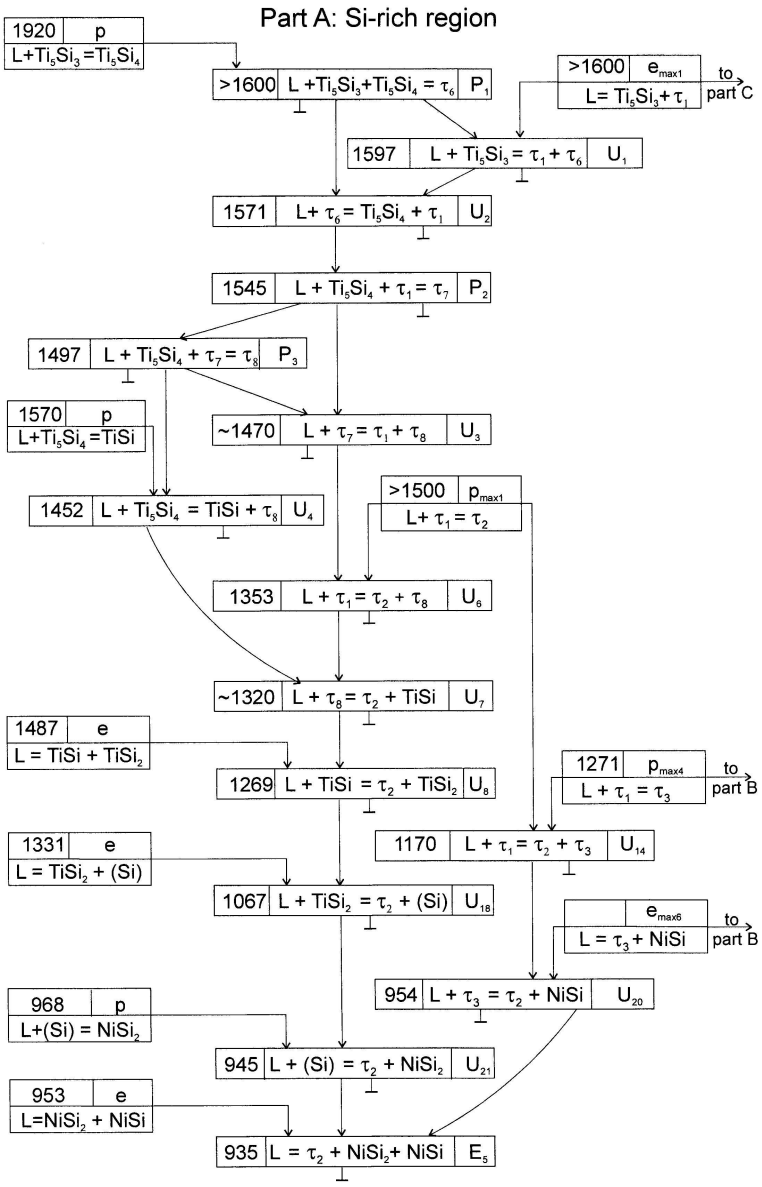

196x292mm (300 x 300 DPI)

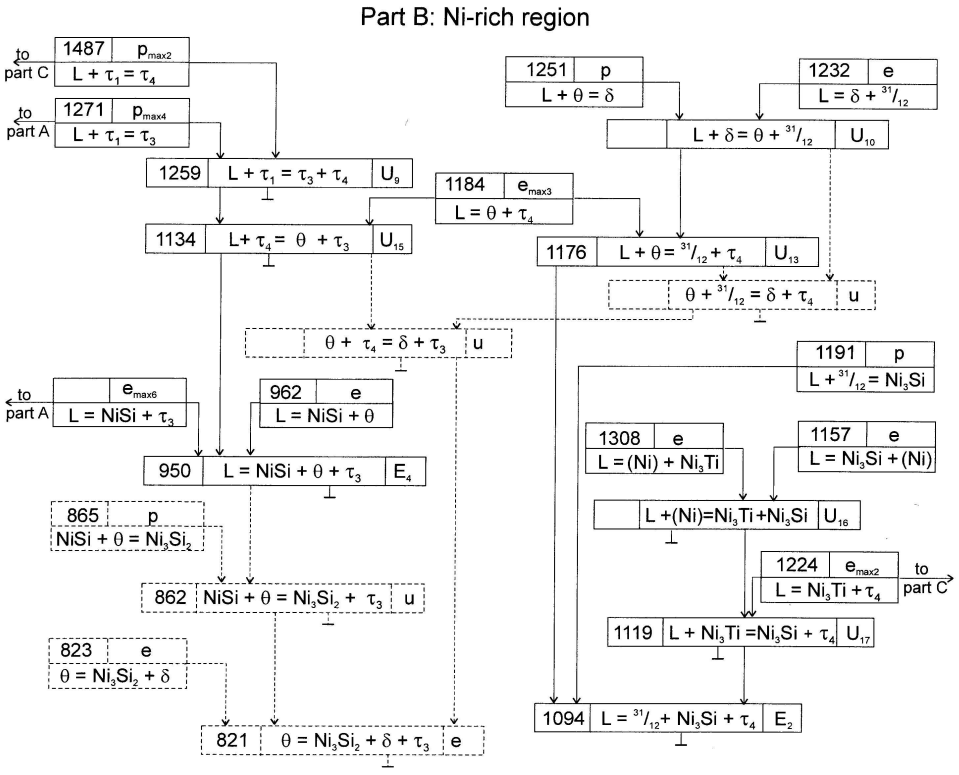

255x205mm (300 x 300 DPI)

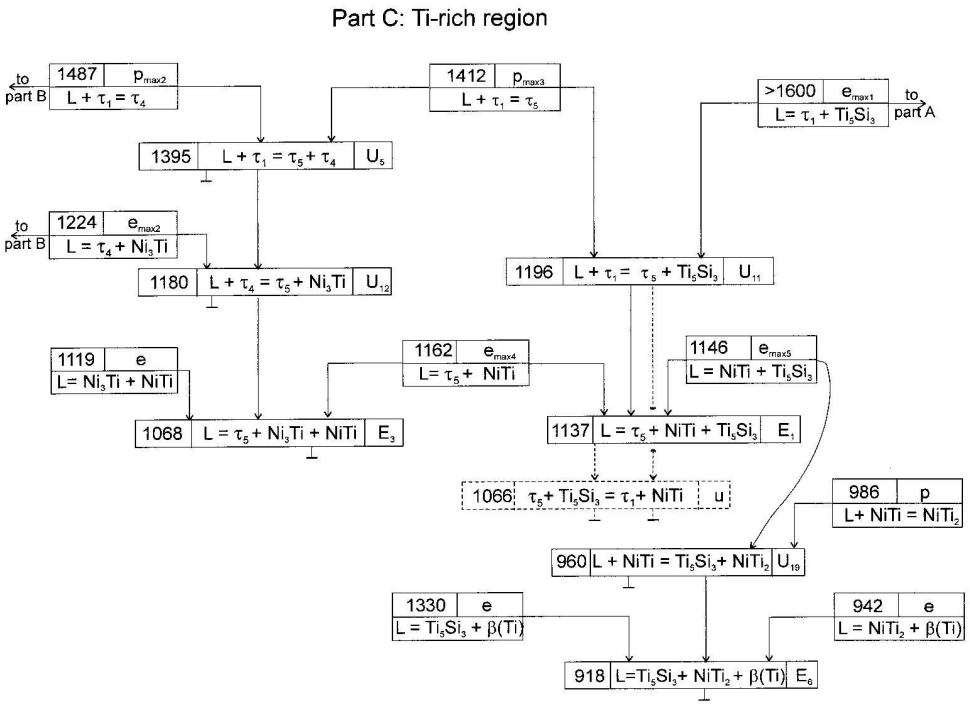

269x201mm (300 x 300 DPI)

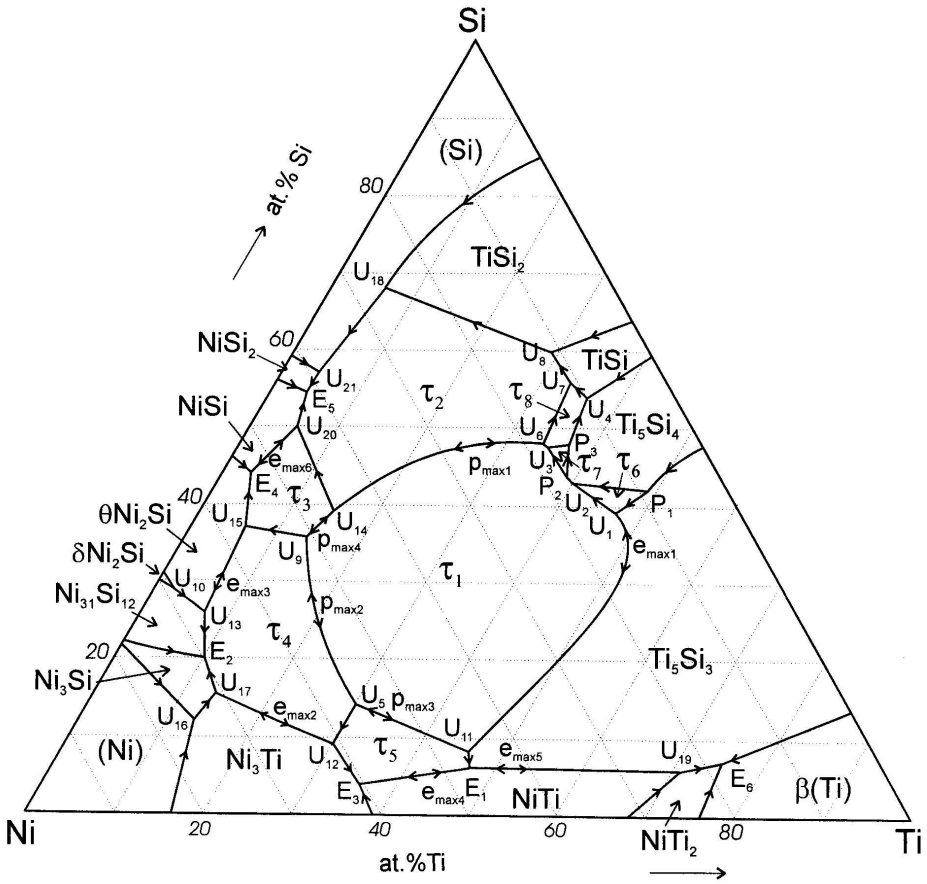

172x166mm (300 x 300 DPI)